UM-HSRI-81-2

Final Technical Letter Report
on NSF Program

OPTIMIZED HIGH-SPEED 35-mm CINERADIOGRAPHIC EQUIPMENT FOR BIOSCIENCES RESEARCH

Grant No. CME-7722578
Grant Period: June 1, 1978 to November 30, 1980

Report to:

Dr. Clifford J. Astill
Program Director, Solid Mechanics Program
Engineering Mechanics Section
Engineering Division
National Science Foundation
Washington, D.C. 20550

Report from:

John W. Melvin, Ph.D., Principal Investigator
Max Bender, M.S., Co-investigator
Biosciences Division
Highway Safety Research Institute
The University of Michigan
Ann Arbor, Michigan 48109

Date: March 2, 1981

Technical Report Documentation Page

1. Report No.	2. Government Accession No.	3. Recipient's Catalog No.
4. Title and Subtitle Optimized High-Speed 35-mm Cineradiographic Equipment for Biosciences Research		5. Report Date March 2, 1981 6. Performing Organization Code
7. Author(s) J. W. Melvin and M. Bender		8. Performing Organization Report No. UM-HSRI-81-2
9. Performing Organization Name and Address University of Michigan Highway Safety Research Institute Ann Arbor, Michigan 48109		10. Work Unit No. 11. Contract or Grant No. CME-7722578
12. Sponsoring Agency Name and Address National Science Foundation Washington, D.C. 20550		13. Type of Report and Period Covered Final Technical Letter Report 6/1/78-11/30/80 14. Sponsoring Agency Code
15. Supplementary Notes		

16. Abstract

A high-speed 16-mm cineradiographic system previously developed at the University of Michigan, Highway Safety Research Institute, for use in biosciences research has been upgraded in capability by 1) increasing the x-ray field to 14-in. by 17-in., 2) incorporating a 35-mm high-speed motion picture to increase resolution, and 3) acquisition of a second x-ray head for three-dimensional x-ray stereophotogrammetric studies. This system now consists of a 35-mm Photosonics 4B camera, capable of 2500 frames per second, which views a 2-in. diameter output phosphor of a high-gain, 4-stage, magnetically focused image intensifier tube, gated on and off synchronously with the motion picture camera. A lens optically couples the input photocathode of the image tube to x-ray fluorescent (rare earth) screen images produced by a smoothed d-c x-ray generator of a conventional type. The system is capable of a wide range of magnification ratios.

17. Key Words biomechanics biosciences x-ray image intensification high-speed x-ray cineradiography	18. Distribution Statement

19. Security Classif. (of this report)	20. Security Classif. (of this page)	21. No. of Pages	22. Price
		11	

TO: Dr. Clifford J. Astill
Program Director, Solid Mechanics Program
Engineering Mechanics Section
Engineering Division
National Science Foundation
Washington, D.C. 20550

FROM: John W. Melvin, Ph.D., Principal Investigator
Head, Biomechanics Department
Biosciences Division
Highway Safety Research Institute
University of Michigan
Ann Arbor, Michigan 48109

DATE: March 2, 1981

SUBJECT: Final Technical Letter Report on NSF Program "Optimized High-Speed 35-mm Cineradiographic Equipment for Biosciences Research," Grant No. CME-7722578, Grant Period from 6-1-78 to 11-30-80.

SUMMARY

Primary objectives of this project were: 1) to increase x-ray viewing area, 2) optimize optical characteristics with a high-quality objective lens, 3) incorporate a 35-mm high-speed motion picture camera into the system, 4) obtain a second x-ray head and high-voltage cables for initiation of x-ray stereophotogrammetry studies with the system, and 5) phase the system into on-going programs.

The system now consists of a high-speed 35-mm motion picture camera, capable of operating at 2500 frames per second, which views a 2-inch diameter output phosphor of a high-gain, four stage magnetically focused image intensifier tube to x-ray images produced on a fluorescent screen by a smoothed direct-current x-ray generator. The system is now more adaptable to a variety of experimental requirements in biomechanics research because 1) a new mechanical structure incorporating a larger bellows has been fabricated which provides a greater range of variation in x-ray viewing area, and 2) the calcium tungstate fluorescent screen has been replaced with a rare earth gadolinium oxysulfide screen, 3M TRIMAX-12, which has four times the light output of calcium tungstate for similar experimental conditions and radiographic factors. The rare earth screen improvement factor allows greater flexibility in choices of experimental geometry, kilovoltage, and current.

Operation and Performance of the High-Speed Cineradiographic System

Its method of operation is as follows: an x-ray fluorescent screen shadowgraph of an impact event is imaged by the objective lens onto the input photocathode of the image intensifier. The x-ray shadowgraph on the fluorescent screen varies continuously in spatial distribution and in time. When the camera shutter is in an open position, the image tube is turned on to allow image light amplification, and when the shutter is in a closed position, the image tube is turned off. This procedure for synchronously gating the image tube with the camera was adopted to 1) reduce noise integration in the output phosphor, 2) to lower the duty cycle of tube operation to allow for higher x-ray input for comparatively thick biological material as encountered in human cadavers, and 3) to protect and conserve the image intensifier tube in general from drawing current when no information is being transmitted to recording film.

A schematic diagram of a representative impact experiment with application of the system is shown in Figure 1. Activation of the impactor driving unit starts an automatic sequence of timed events which includes x-ray turn-on, motion picture camera start, gated image intensifier tube operation in synchronization with the camera shutter, the impact event, and shut-down of the system, all occurring in approximately 200 ms. A magnetic pick-up element senses onset of the impactor head motion and provides a system activation pulse to the x-ray control unit. The x-ray control unit then distributes signals to the x-ray generator and high-speed motion picture camera, which then initiates image intensifier tube operation in gated mode.

Components of the imaging elements of the system are shown in Figures 2 and 3. Figure 2 shows the 14-in. by 17-in. rectangular magnesium alloy plate which supports the gadolinium oxysulfide fluorescent screen inside the bellows. The cylindrical structure contains the electron focusing magnet. The four-stage image intensifier tube lies in the center of the cylindrical magnet housing along its longitudinal axis. The 35-mm high-speed motion picture camera views the output phosphor of the image tube, as shown in Figure 3. The imaging elements in Figure 2 are positioned in a Unistrut structure which

FIGURE 1. Schematic Diagram of Impact Experiment

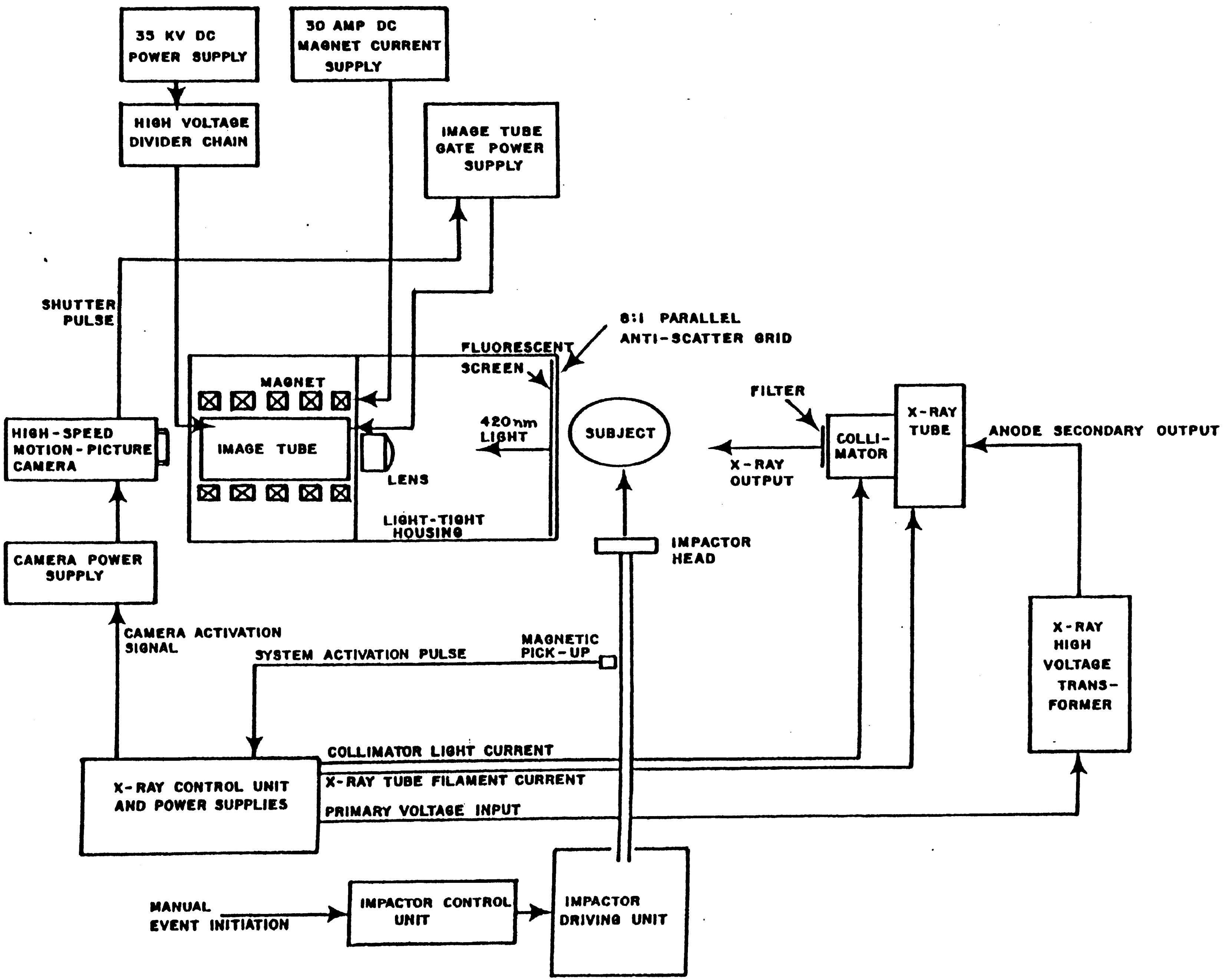

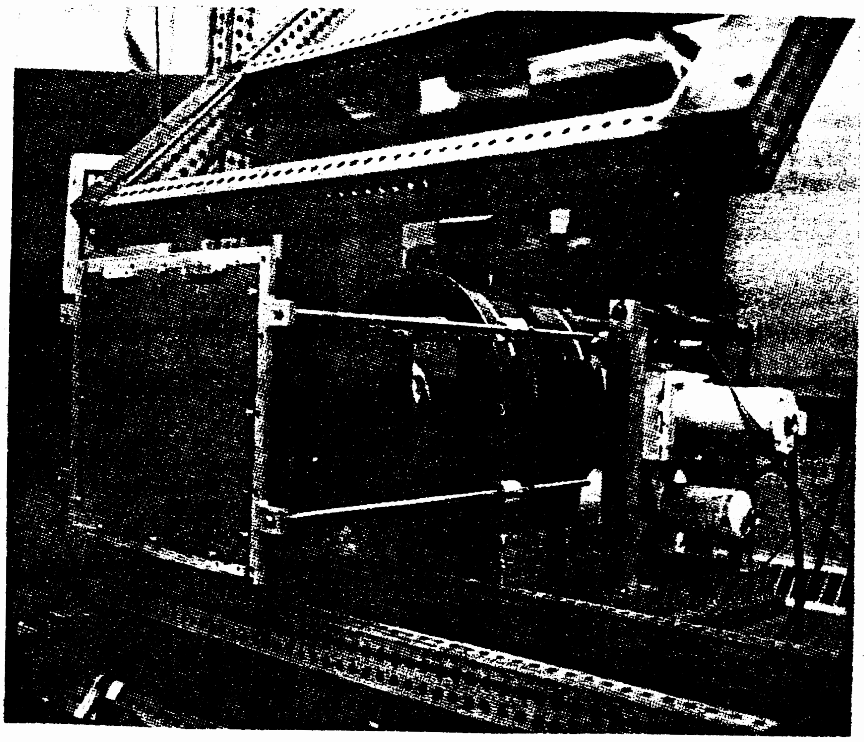

Figure 2

High-Speed 35-mm Cinematographic X-Ray Imaging Elements

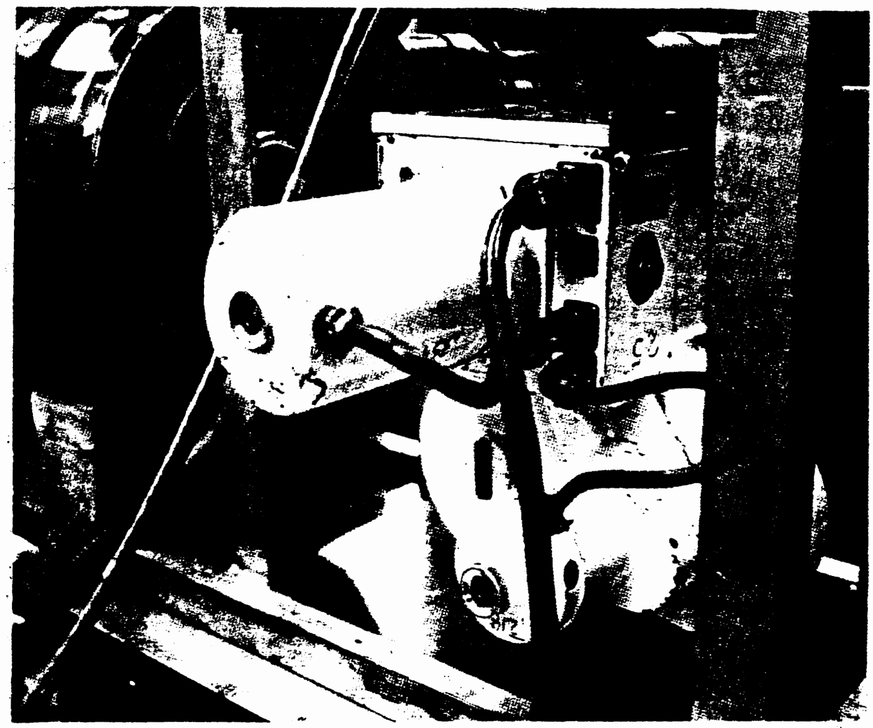

Figure 3

35-mm Photosonics 4B High-Speed Motion Picture Camera holds a 16-mm high-speed motion picture camera and lights, to obtain an optical film record simultaneously with the dynamic x-ray image record.

Figure 4 shows the control console and associated electronics, which consist of the d-c high-voltage power supply at the left, the high-voltage divider, the image tubing gating supply, and the magnet current power supply. Image tube gain, gate pulse width, and magnetic focus are controlled from the console.

Gating pulse shape is shown in the upper trace of Figure 5. The peak amplitude of this signal is proportional to a positive 3.3 Kv gate pulse, applied to the input photocathode of the image intensifier tube, which is normally at ground potential when the tube is in a conducting state. The 3.3 Kv gate pulse raises the normally grounded photocathode to approximately the same potential as the first dynode ring in the first stage of the image tube. This produces a nearly zero potential gradient, and therefore no photo-electron flow between input photocathode and the first dynode, shutting the image tube off. When the gate pulse voltage falls to zero, the photocathode is again in its normal ground state and tube conduction occurs. In this example the tube was on for nearly 400 μs, and off for about 600 μs, at 1 KHz pulse repetition rate. Pulse width is controllable, and is normally set at a width of 225 μs to overlap camera shutter open time of 200 μs at 1000 frames per second. The gate pulse is an excellent approximation to a square wave, with a rise time of approximately 50 μs, without ringing, overshoot, or variation in required voltage level.

Light output decay time is shown in the lower trace, where the abscissa is in units of 0.2 ms/div., time running to the right. The image tube has three fast phosphors with a decay time of 5 μs each, and a P-11 output phosphor with a decay time of nominally 90 μs. Decay time of the chain is the convolution of all of them, but approximately 200 μs is seen on the lower trace; this also includes interdynode capacitance of the image tube and time constant of the photomultiplier measurement circuitry. The dominant contributor to this decay time is the P-11 phosphor, which actually does not have a unique time constant, but varies proportionally according to excitation level and also to time duration of excitation. When the gate pulse width

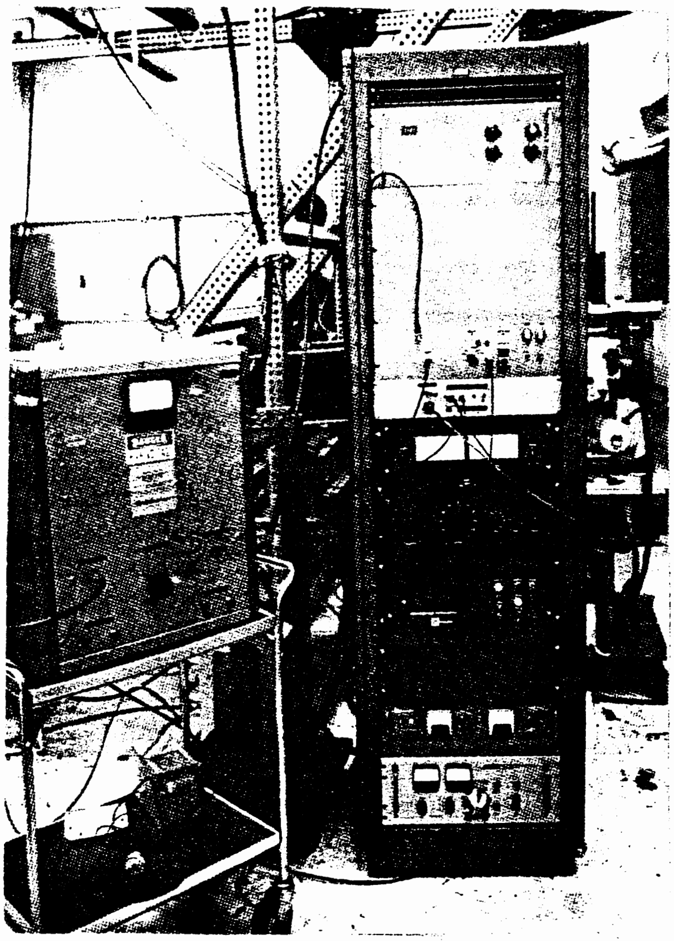

Figure 4

Control Console and Associated Electronics

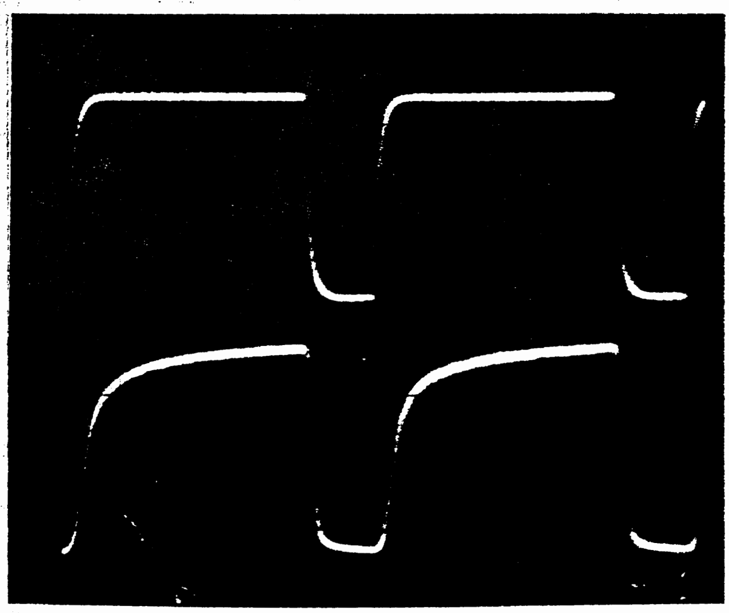

image tube OFF

image tube ON

Figure 5

Synchronization of Image Tube Light Output with Image Tube Gating Pulse

Upper trace: gating pulse, 0.2 ms/div; frequency 1 KHz

Lower trace: PM tube record of image tube light output is narrowed to approximately 200 μs, decay time becomes smaller, which allows a higher x-ray input level necessary for relatively dense subjects. The light output in the example shown is seen to fall to nearly zero before the onset of a successive gate pulse.

Optical verification of resolution performance is shown in Figure 6. A 14-in. x 17-in. video test pattern chart, illuminated by d-c incandescent light inside the bellows, was viewed by the image intensifier in gated operation at 1 KHz pulse repetition rate; pulse width was 293 μs; optical magnification ratio was 1:23, i.e., the 2.75-in. by 2.75-in. vertical line grid in the center of the pattern was reduced to 0.75-in. by 0.75-in. in the Polaroid photograph.

Figure 7 shows a greatly magnified image of the grid at at overall magnification ratio of 1:1, which demonstrates the variability of the system in meeting diverse experimental requirements by different users of the equipment.

Magnetically focused image intensifiers display a characteristic spiral, or S-type distortion, because the magnetic field is not perfectly uniform. This is seen at the edges of the image in Figures 6 and 7 as displacement from linearity of the image of a line. These tubes provide least distortion and highest edge resolution compared to electrostatically focused tubes, which give a pincushion type distortion and defocusing at its edges. Error correction for either type of distortion in quantitative measurements is straight-forward.

Applications to Biomechanics Research

Current injury assessment research is aimed at four regions of the human body: the head, neck, thorax, and knee. This system in its earlier configuration has been applied to all of these regions in various experimental programs at HSRI. Each subject specimen presents a different problem in choosing x-ray factors, targeting, and geometry so that optimum density and contrast will be obtained in the film. Targeting structures of interest involves selection and placement of radiopaque materials to provide contrast enhancement.

An example of image quality obtained with the optimized system is shown in Figure 8, which is an x-ray intensified image of a knee joint, a portion of the femur, and the bones of the lower leg. Nine

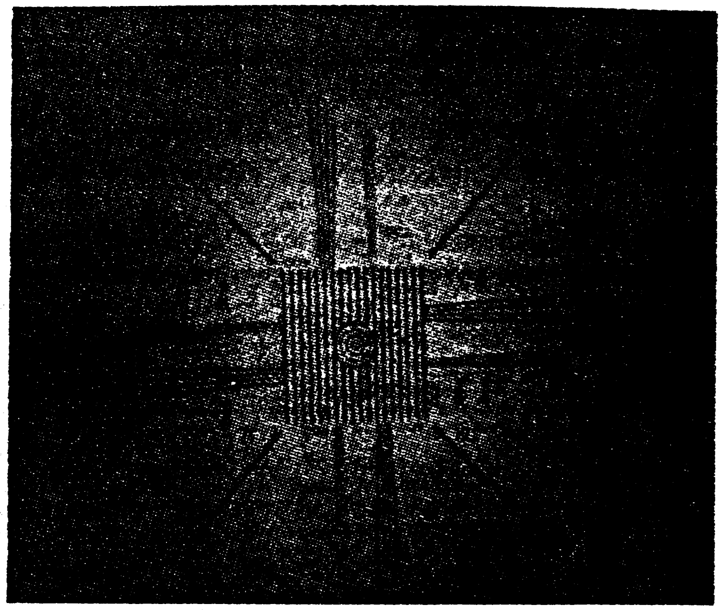

Figure 6

Intensified Image of 14-in. x 17-in. Resolution Chart

(overall) Magnification Ratio: 1:23

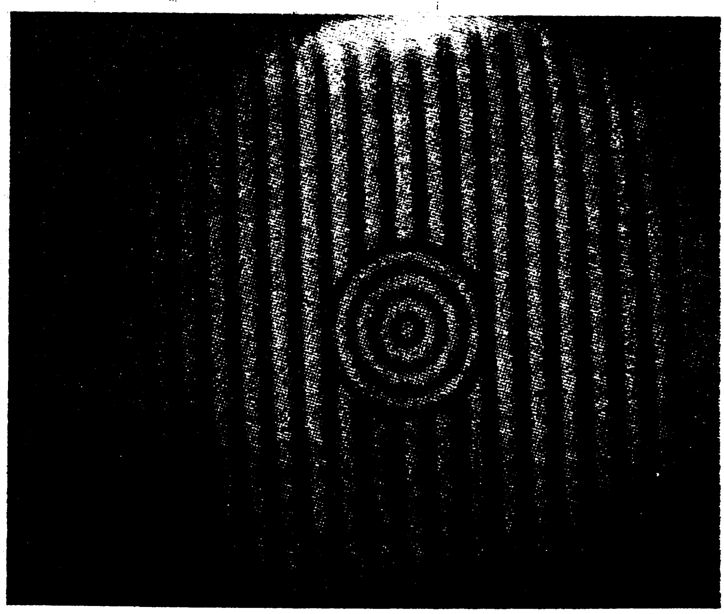

Figure 7

Intensified Image of Magnified 14-in. x 17-in. Resolution Chart

(overall) Magnification Ratio: 1:1

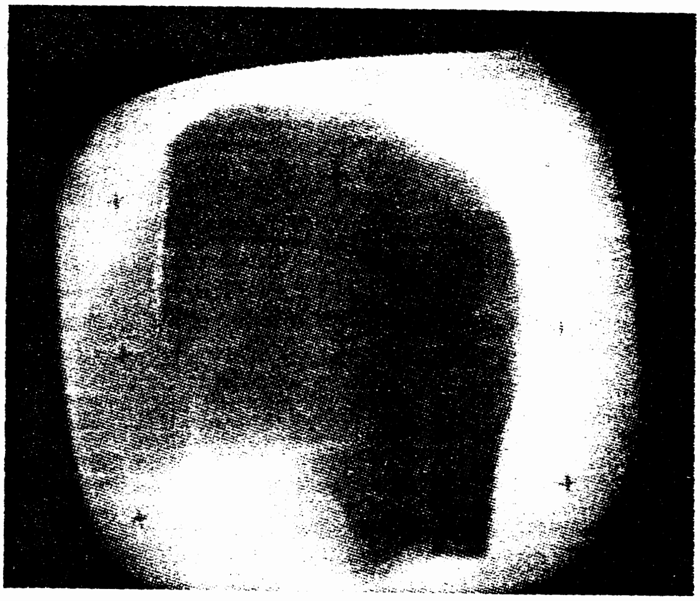

Figure 8

X-Ray Intensified Image of Knee

(still)

Focal spot distance to knee: 33.5-in.

Focal spot distance to screen: 38-in.

X-Ray factors: 90 kVp, 50 ma, 1/30 s.

Dimensions of vertical wires on femur, from left to right, 0.094-in. and 0.047-in.

fiducial marks made of lead are embedded in the magnesium alloy plate which supports the fluorescent screen. These are seen in Figure 8 as an array of crosses, to serve as registration indices from one motion picture frame to another in quantitative analysis. The image of the knee-joint is somewhat magnified because the x-ray source focal spot distance to the knee-joint was 33.5-in., while the focal spot distance to the screen was 38-in. The femur is seen to be targeted with lead wires and pellets. Their diametric dimensions are, from left to right: 0.094-in., 0.047-in., 0.231-in., 0.184-in., and 0.257-in., respectively.

Density variation in bone is clearly observable, as well as all of the parts of the knee-joint and their relationship. Another noteworthy aspect of this image example is that an anti-scatter grid was not used. This points out the lower x-ray scattering property of the rare earth screen.

In conclusion, the optimized high-speed 35-mm cineradiographic system is regarded as a successful equipment facility with the potential for three dimensional motion analysis when the now acquired second x-ray head is phased into the system for x-ray stereophotogrammetry.

List of publications based all or in part on the general high-speed x-ray cinematographic system acquired with NSF support:

1. M. Bender, W. L. Rogers, and J. W. Melvin, "HSRI High-Speed X-Ray Cinematographic System for Biomechanics Research," Effective Utilization of Photographic and Optical Technology to the Problems of Automotive Safety, Emissions and Fuel Economy, Society of Photo-optical Instrumentation Engineers, Palos Verdes, CA., 1975.

2. M. Bender, J. W. Melvin, and R. L. Stalnaker, "A High-Speed Cineradiographic Technique for Biomechanical Impact," Proceedings of Twentieth Stapp Car Crash Conference, Society of Automotive Engineers, Warrendale, PA., 1976.

3. R. L. Stalnaker, J. W. Melvin, G. S. Nusholtz, N. M. Alem, and J. B. Benson, "Head Impact Response," Proceedings of Twenty-first Stapp Car Crash Conference, Society of Automotive Engineers, Warrendale, PA., 1977.

4. R. L. Stalnaker, M. Bender, and J. W. Melvin, "Safety Helmet-Head Interaction Study Using High-Speed Cineradiography," Final Report UM-HSRI-77-48 to National Institute of Occupational Safety and Health, Morgantown, W.V., 1977.

5. R. H. Culver, M. Bender, R. L. Stalnaker, J. W. Melvin, and D. C. Viano, "Feasibility of Investigating Mechanisms of Aortic Trauma Using High-Speed Cineradiography," UM-HSRI-77-53, Final Report to General Motors Research Laboratories, General Motors Corporation, Warren, MI., December, 1977.

6. R. H. Culver, M. Bender, R. L. Stalnaker, and J. W. Melvin, "Evaluation of Intrathoracic Response Using High-Speed Cineradiography," Proceedings of the Sixth Annual New England Bioengineering Conference, Univ. of Rhode Island, Kingston, R.I., March 23 - 25, 1978, Pergamon Press, New York, N.Y., 1978.

7. M. Bender and J. W. Melvin, "High-Speed X-Ray Cinematography at HSRI," HSRI Technical Review, January-February 1979, The University of Michigan, Ann Arbor, MI.

8. G. S. Nusholtz, J. W. Melvin, N. M. Alem, "Head Impact Response Comparisons of Human Surrogates," Proceedings of Twenty-third Stapp Car Crash Conference, Society of Automotive Engineers, Warrendale, PA., 1979.

9. R. Matteson, L. W. Schneider, Gary Czupinski, Leigh Peck, and M. Bender, "A Cineradiographic Analysis of Needle Penetration," UM-HSRI-80-8, Report to Becton-Dickinson Corporation, East Rutherford, N.J., August, 1980.

10. G. S. Nusholtz, J. W. Melvin, G. Mueller, J. R. MacKenzie, and R. Burney, "Thoraco-Abdominal Response and Injury," Proceedings of Twenty-fourth Stapp Car Crash Conference, Society of Automotive Engineers, Warrendale, PA., 1980.